13

Wavelet Evolution and Flexible Algorithm for Wavelet Segmentation, Edge Detection and Compression with Example in Medical Imaging

Igor Vujović[1], Ivica Kuzmanić[1], Mirjana Vujović[2], Dubravka Pavlović[3] and Joško Šoda[4]

[1] *University of Split, Maritime Faculty*
[2]*Private practice of occupational health, Ploče*
[3]*Health Centre Ploče, Radiological Department*
[4]*University of Split*
Faculty of Electrical Engineering, Mechanical Engineering and Naval Architecture
Croatia

1. Introduction

A central goal in signal analysis is to extract information from signals that are related to real-world phenomena. Examples are the analysis of speech, images and signals in medical or geophysical application, to name it a few. One reason to analyze such signals is to achieve better understanding of the underlying physical phenomena. Another is to find compact representations of signals which allow compact storage or efficient transmission of signals through real-world environments. The methods of analyzing signals are wide spread and range from classical Fourier analysis to various types of linear time-frequency transforms and model-based and non-linear approaches.

Wavelet methods in image processing, analysis, compression, superresolution and enhancement are widely present in many researches such as biomedical applications, technology, industry, robotics, space explorations, military, etc. Wavelets have evolved over years. The theory of the first generation of wavelets (FGW) is originated on filter banks theory which includes classical Fourier analysis techniques (Mallat, 1999; Vetterli & Kovačević, 1995). Classical Fourier analysis is an irreplaceable tool in many engineering fields for years, and was solved many problems of linear-time invariant systems that include finding a spectrum of stationary signals (Proakis & Manolakis, 2006). For a non-stationary character of measured signal that spectral content is changing over time, classical Fourier analysis has shown weaknesses. The Fourier analysis only partly solves mentioned problems, a new approach is needed which will give a new insight into signal properties in a different way. Proposed new approach has been time-frequency analysis, i.e. a signal representation in time-frequency plane. The most popular time-frequency analyses are the short-time Fourier Transform (STFT) which is also called the classical method of time-frequency analysis and Wavelet Transform (WT or FGW) which is also called the time-scale analysis (Mertins, 1999). Wavelet transform brought flexible windows for analysis. The

Source: Vision Systems: Segmentation and Pattern Recognition, ISBN 987-3-902613-05-9,
Edited by: Goro Obinata and Ashish Dutta, pp.546, I-Tech, Vienna, Austria, June 2007

second generation wavelet transform (SGW) is a newly proposed wavelet transform where the filters are not designed explicitly, but the transform consists of application of the lifting scheme. The sequence of lifting steps could be converted to a regular discrete wavelet transform, but it is unnecessary because both design and application is made via the lifting scheme (Sweldens, 1996, Daubechies & Sweldens, 1998). Measured signals of the main interest are not periodic. The area of the interest is not always finite and one-dimensional signals are not always uniformly sampled. At two or more dimensions (i.e. irregular surface) even more complicated situation arises. The FGW localize time-frequency well. Developed fast algorithms for FGW would be adopted in some way, by giving up dilatations and translation. Second generation wavelets (SGW) have updates and predictions instead of filter representation, the SGW have polyphase representation (Jansen & Oonicx, 2005). Factorization by lifting steps was a new approach, which introduces a new quality in computation of wavelet and scaling coefficients. Lifting transform can be applied to FGW as well. Then computationally interesting polyphase matrixes are obtained, which become triangle or scalar for the FGW. It is possible to construct FGW on the SGW settings and vice versa, but the SGW are so powerful that there is no need for transformation of SGW to FGW. The nanotechnology is the reason for improvement of SGW. Namely, research of nanostructures needs better characterization of atoms. The third generation wavelets (TGW) are proposed in (Xiao 2003, Jiang 2003, Vujović et al., 2006a; Vujović et al., 2006b). Wavelets have showed they are unlike numerous techniques which only remain popular for a short period of time – and they demonstrated ability to adopt.

Wavelets have shown great potential and abilities in various technical applications (Šoda, 2005). Nowadays, they are topical in image processing for on and off-line applications (computer vision, robot vision, security systems, etc).

Object segmentation through human-robot interactions in the frequency domain (Arsenio, 2003) was based on segmentation of windowed FFT. But, windowed FFT can be easily transformed to WT. Segmentation of colour images with fast wavelet transform is presented in (Chan et al, 2005).

Interesting application of wavelets for progressive edge detection and edge defection prediction has been developed in the XXI century (Abbas & Alsultanny, 2005). It exploits the observation that wavelet decomposition at higher levels degrades the image in the sense of leaving almost nothing but edges. However, their progressive and predictive detection is based on simple ones. It is not preferable in nowadays science, because everyone tries to find more and more complicated methods. Authors of this chapter evoke for such approach on many occasions. It is the best when you get satisfactory results with simple and elegant methods.

Compression of data, including image compression, is one of the most outstanding applications of wavelets. Some older examples are in references (Heer & Reinfelder, 1990; Said & Pearlman, 1996; Calderbank et al., 1997; Akay, 1998). Nowadays, influence of wavelets in many compression applications is being researched, i.e. in biomedical imaging (Vujović, 2004; Vujović et al, 2003.). Powerful compression possibilities of wavelets have been exploited in many applications, off and on-line, for single images and for image sequences. Wavelets are incorporated in JPEG-2000 standard as well and security (Boles, 1998; Grosbois, 2003; Dai & Yuen, 2006). However, their ability in denoising and compression often depend on thresholding. Automated methods for thresholding are of great interest for wavelets.

Wavelet compression ability gave rise to the idea of reverse process using them for obtaining higher resolutions. A great interest exists for such superresolution issues in the military, security, police, etc., as well as scientific community (Candocia, 1998; Nguyen, 2000; Bose, 2003; Borman, 2004; Chappalli & Bose, 2005).
This chapter describes an interesting approach in wavelet usage for image processing. Superresolution is used for image enhancement before compression by downsampling. The entire process is performed on the wavelet coefficients.

2. Wavelet generations

Heisenberg principle is interesting in the time-frequency domain, because it states that there is a limitation of measurement for time and frequency at the same time. If we can measure time and frequency infinitely precisely, the product of time and frequency is bounded according to Heisenberg principle. Actually, Heisenberg states that we can measure only time or only frequency with infinite precision. The product of time interval, Δt, and frequency interval, Δf, is constant.
This window is area in which it is presumed that amplitude is unchanged (of course, that is only a rough approximation in practice, which introduces error). The consequence of such window size is the worst resolution of time at high frequencies and the worst resolution of frequency at lower frequency range. Wavelet analysis is a multiresolution analysis (MRA): rectangles are vertically elongated at high frequencies, which means better time resolution and horizontally elongated at low frequencies, which means better frequency resolution. This limitation is better described by tiling scheme presented in Fig. 1.

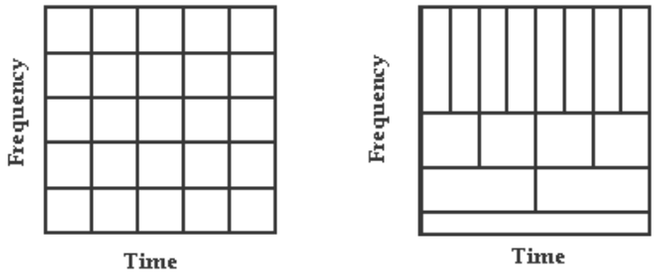

a) *b)*

Fig. 1. Tiling scheme: a) STFT – same window for frequency and time for high and low frequency range, b) MRA – windows have the same surface, but different edge lengths

Once a window has been chosen for the STFT, then the time-frequency resolution is fixed over the entire time-frequency plane since the same window is used at all frequencies. To overcome the resolution limitations of the STFT one can imagine letting the resolution Δt and Δf vary in time-frequency plane in order to obtain a multiresolution analysis. The analysis filter bank is then composed of band pass filters with constant relative bandwidth, so called "constant Q-analysis".
The integral transform is one of the most important tools in signal theory (Mertins, 1999). Fourier transform is the best known example, but there are many other transforms, such as

Hartley and Hilbert, that can be derived from the integral signal representation. In the following, we will briefly outline the basic concept of integral transform.
The basic idea of an integral representation is to describe a signal *x(t)*, that is integrable in Lebesque sense and closed on $L_2(R)$, via its density *X(s)*, that is also integrable in Lebesque sense and closed on $L_2(R)$, with respect to arbitrary kernel *φ(t,s):*

$$x(t) = \int_S X(s)\varphi(t,s)ds \quad t \in T \subseteq L_2(R) \tag{1}$$

Using analogous approach, and denoting *θ(s,t)* as reciprocal kernel, the density *X(s)* can be calculates in the form:

$$X(s) = \int_T x(t)\theta(s,t)dt \quad s \in S \subseteq L_2(R) \tag{2}$$

By substituting (2) in (1) it can be obtained:

$$x(t) = \int_T x(\tau) \int_S \theta(s,\tau) \cdot \varphi(t,s) \cdot ds \cdot d\tau \tag{3}$$

In order to state the condition for the validity of (3) in a relatively simple form the so called Dirac impulse *δ (t)* is required. A generalized function *x (t)* then can be presented as follows:

$$x(t) = \int_T x(\tau) \cdot \delta(t-\tau) \cdot d\tau \tag{4}$$

Equations (3) and (4) show that the kernel and reciprocal kernel must satisfy:

$$\int_S \theta(s,\tau) \cdot \varphi(t,s) \cdot ds = \delta(t-\tau) \tag{5}$$

Similarly, by substituting (1) in (2), and then applying the same approach as above, implies:

$$\int_S \varphi(t,\sigma) \cdot \varphi(s,t) \cdot dt = \delta(s-\sigma) \tag{6}$$

A special category is that of self-reciprocal kernels. That corresponds with orthonormal bases in the discrete case and satisfies:

$$\varphi(t,s) = \theta^*(s,t) \tag{7}$$

Transforms that contain a self-reciprocal kernel are also called unitary transforms.
Let *x (t)* be a real or complex-valued continuous-time signal which is integrable in Lebesque sense. For such signals the Fourier transform exists:

$$X(\omega) = \int_{-\infty}^{+\infty} x(t) \cdot e^{-j \cdot \omega t} \cdot dt \tag{8}$$

Here $\omega = 2 \cdot \pi \cdot f$ and *f* is the frequency in Hertz.
If *X (ω)* is also integrable in Lebesque sense, *x (t)* can be reconstructed from *X (ω)* via the inverse Fourier transform:

$$x(t) = \frac{1}{2 \cdot \pi} \int_{-\infty}^{+\infty} X(\omega) \cdot e^{j \cdot \omega t} \cdot d\omega \tag{9}$$

The kernel used is:

$$\varphi(t, \omega) = \frac{1}{2 \cdot \pi} e^{j \cdot \omega t} \quad T \in \langle -\infty, +\infty \rangle \tag{10}$$

and for reciprocal kernel we have

$$\theta(\varpi, t) = e^{-j \cdot \omega t} \quad S \in \langle -\infty, +\infty \rangle \tag{11}$$

From the equations (10) and (11) it can be seen that trigonometric functions form a basis that span the Fourier space. Trigonometric functions satisfy (5), i.e. they form the orthonormal basis on Fourier space. Also, the support of trigonometric functions is infinite in the time domain, which means that localization in the time is poorly determined, i.e. time resolution is poor. Unlike to time domain, in frequency domain Fourier transform gives perfect resolution, since trigonometric functions can be described with Dirac impulse. Heisenberg principle of uncertainty does apply here too.
The wavelet transform *W (a, b)* of a continuous-time signal x (t) is defined as:

$$W(a,b) = |b|^{\frac{-1}{2}} \cdot \int_{-\infty}^{+\infty} x(t) \cdot \psi^*(\frac{t-a}{b}) \cdot dt \tag{12}$$

Thus, the wavelet transform can be viewed, and is computed, as the inner product of *x (t)* and translated and scaled versions of a single function *ψ (t)*, the so-called wavelet. A wavelet function *ψ (t)* is a function of zero average. If *ψ (t)* is considered to be a bandpass impulse response, then the wavelet analysis can be understood as a bandpass analysis. By varying scaling parameter *b* the centre frequency and the bandwidth of the bandpass are influenced. The variation of *a* simple means a translation in time, so for a fixed *b* the transform (12) can be seen as a convolution of *x (t)* with the time-reversed and scaled wavelet

$$W_x(t,b) = |b|^{\frac{-1}{2}} \cdot x(t) * \psi_b(t), \quad \psi_b(t) = \psi^*(\frac{-t}{b}) \tag{13}$$

Time and frequency resolution of WT depends of *b*. For high analysis frequencies, good time localization but poor frequency resolution can be achieved. On the other hand, for low analysis frequencies, good frequency but poor time resolution can be achieved. When using a transform in order to get better insight into the properties of a signal, it should be ensured that the signal can be perfectly reconstructed from its representation. Otherwise the representation may be completely or partly meaningless. For WT the condition that must be met in order to ensure perfect reconstruction is:

$$C_\psi = \int_{-\infty}^{+\infty} \frac{|\psi(\omega)|^2}{|\omega|} \cdot d\omega < \infty \tag{14}$$

Where *Ψ (ω)* denotes FT of the wavelet. This condition is known as the admissibility condition for the wavelet *ψ (t)*.

Discrete wavelet transform (DWT) is based on multirate filter banks theory. There are two possible ways to obtain coefficients of DWT, by applying one of the two MRA algorithms, or by sampling CWT coefficients. The following dyadically arranged sampling points are used:

$$b_m = 2^m, \quad a_{mn} = b_m \cdot n \cdot T = 2^m \cdot n \cdot T \tag{15}$$

This yields the values $W_x(a_{mn}, bm) = W_x(2^m nT, 2m)$. Furthermore,

$$\psi_{mn}(t) = |b_m|^{\frac{-1}{2}} \cdot \psi\left(\frac{t - a_{mn}}{b_m}\right) = 2^{\frac{-m}{2}} \cdot \psi(2^{-m} \cdot t - nT) \tag{16}$$

Finally, (12) becomes:

$$W_x(a_{mn}, b_m) = W_x(2^m nT, 2^m) = \langle x, \psi_{mn} \rangle \tag{17}$$

The values $\{W_x(2^m nT, 2^m),\ m,n \in R\}$ form the representation of $x(t)$ with the respect to the wavelet $\psi(t)$ and the chosen grid. We cannot assume that any set $\psi_{mn}(t),\ m,\ n \in R$ allows reconstruction of all signals $x(t) \in L_2(R)$. For this a dual set $\tilde{\psi}_{m,n}(t)$, $m,\ n \in R$ must exist, and both set must span $L_2(R)$, any $x(t) \in L_2(R)$ can be written as:

$$x(t) = \sum_{m=-\infty}^{\infty} \sum_{n=-\infty}^{\infty} \langle x, \psi_{mn} \rangle \cdot \tilde{\psi}_{mn}(t) \tag{18}$$

Alternatively, x(t) can be written:

$$x(t) = \sum_{m=-\infty}^{\infty} \sum_{n=-\infty}^{\infty} \langle x, \tilde{\psi}_{mn} \rangle \cdot \psi_{mn}(t) \tag{19}$$

For a given wavelet $\psi(t)$, the possibility of perfect reconstruction is dependent on the sampling interval T. If T is chosen very small i.e. we have oversampling, the values $\{W_x(2^m nT, 2^m),\ m,n \in R\}$ are highly redundant, and reconstruction is very easy. Then the functions $\psi_{mn}(t),\ m,\ n \in R$ are linearly dependent, and an infinite number of dual sets $\tilde{\psi}_{mn}(t)$ exists. The question of whether a dual set $\tilde{\psi}_{mn}(t)$ exists at all can be answered by checking two frame bounds A and B. It can be shown that the existence of a dual set and the completeness are guaranteed if the stability condition:

$$A \cdot \|x\|^2 \le \sum_{m=-\infty}^{\infty} \sum_{n=-\infty}^{\infty} |\langle x, \psi_{mn} \rangle|^2 \le B \cdot \|x\|^2 \tag{20}$$

with the frame bounds $0 < A \le B < \infty$ is satisfied (Mertins, 1999). The higher the frame bounds are, the smaller is the reconstruction error. In the case of a tight frame, A = B, perfect reconstruction with $\tilde{\psi}_{mn}(t) = \psi_{mn}(t)$ is possible. With MRA and wavelets resolution is degraded or enhanced by necessity. MRA trades off between both resolutions.

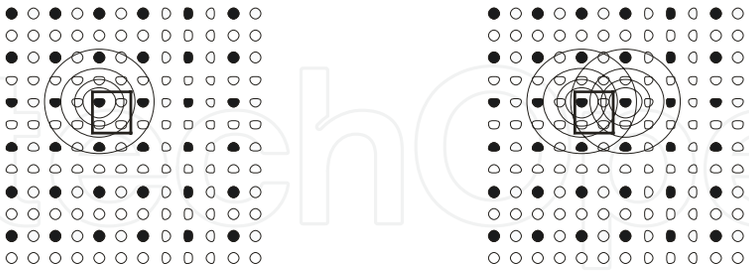

a) b)

Fig. 2. a) Interaction of the single pixel to the neighbours, b) interaction between two pixels

When talking about images, WT is two-dimensional. The error in image analysis begins with digitalization. Namely, in sensors. Sensors are not continuous. They are usually CCD arrays. The basic starting point is that light has the same frequency and amplitude over a single CCD cell. It is not true. However, it is often a good enough approximation. To obtain better image quality, more details must be obtained by some form of interpolation method.
Interpolation method can be primitive and simple or more sophisticated. Transition from a low-resolution image to a more detailed (high resolution image) does not depend only on the observed pixel, but also on its neighbouring pixels. But how can the neighbouring pixels be accounted for? I.e. are the pixels in diagonal positions less influenced by the observed pixel and vice versa? The solution is in introduction of weights for pixels. If this is performed on FGW coefficients we call the product "intuitive wavelets":

$$W(a,b) \cong \int \rho(a,b)x(t)\cdot\psi^{*}_{j,k}(t)dt = d_{j,k} \tag{21}$$

where ρ(a, b) is the weight function. Observe that if ρ(x, y) is the weight of the pixel, then this is propagating through WT into ρ(a, b), because the weight function is just a set of constants. Introduction of weights can be interpreted as primitive type of SGW. Therefore it can be said that this is the SGW on the FGW settings. However, SGW can be introduced for discrete signal and linear filters, which perform perfect reconstruction in z-domain.
Polyphase representation of signal $X(z) = X_p(z^2) + z^{-1}X_n(z^2)$ where X_p i X_n even and odd samples of the signal x and can be written as:

$$X_p(z) = \sum_k x[2k]z^{-k} \text{ and } X_n(z) = \sum_k x[2k+1]z^{-k}$$

The final result is the polyphase matrix of the system:

$$P(z) = \begin{pmatrix} H_p(z) & G_p(z) \\ H_n(z) & G_n(z) \end{pmatrix} \tag{22}$$

In simulations and numerical experiments, the result is the estimated matrix $\widetilde{P}$ and the error $P - \widetilde{P}$ has to be minimized. Filtering is directly performed on either even or odd samples, which breaks down number of operations by factor 2.

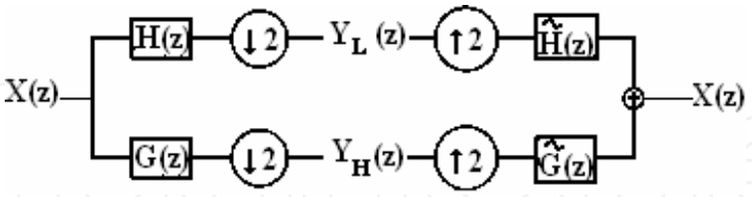

Fig. 3. Perfect reconstruction in Z-domain

The authors propose that FGW and SGW pass the morphology preprocessing in order to emphasize edges. Wavelet coefficients obtained by that manner can be called the third generation wavelets (TGW). This will facilitate further enhancement in different applications. An algorithm for TGW is proposed in (Vujović, Kuzmanić & Vujović, 2006a), but it is not the only way. When talking about TGW, another possibility can be to enhance wavelet coefficient matrixes by i.e. motion field. If stationary image is processed, then quasi-superresolution has to be used.

3. Flexible algorithm

Many algorithms for edge detection, segmentation or compression exist. Some of them are based on wavelets. However, wavelets have some properties which can be used for different operations. The proposed algorithm exploits these properties.

3.1. Wavelet motion field

Let us consider an image sequence $I(p_i, t)$ with $p_i = (x_i, y_i) \in \Omega$ the location of each pixel in the image. The brightness constancy assumption states that the image brightness $I(p_i, t+1)$ is a simple deformation of the image at time t:

$$I(p_i, t) = I(p_i + v(p_i), t + 1) \tag{23}$$

where $v(p_i, t) = (u, v)$ is the optical flow between $I(p_i, t)$ and $I(p_i, t+1)$. This velocity field can be globally modelled as a coarse-to-fine 2D wavelet series expansion from scale L to l (Bruno & Pellerin, 2002):

$$V_\theta(p_i) = \sum_{k_1,k_2=0}^{2^L-1} c_{L,k_1,k_2}\Phi_{L,k_1,k_2}(p_i) + \\ + \sum_{j\geq L}^{l}\sum_{k_1,k_2=0}^{2^j-1}\left[d^H_{n,k_1,k_2}\Psi^H_{j,k_1,k_2}(p_i) + d^V_{n,k_1,k_2}\Psi^V_{j,k_1,k_2}(p_i) + d^D_{n,k_1,k_2}\Psi^D_{j,k_1,k_2}(p_i)\right] \tag{24}$$

where $\Phi_{L,k_1,k_2}(p_i)$ is the 2D scaling function at scale L and Ψ^H_{j,k_1,k_2}, Ψ^V_{j,k_1,k_2}, Ψ^D_{j,k_1,k_2} are wavelet functions which represent horizontal, diagonal and vertical directions. These functions are dilated by 2^j and shifted by k_1 and k_2. The solution can be found by usage of some error function and minimization, i.e. (Bruno & Pellerin, 2002; Bruno & Pellerin, 2001):

$$E = \sum_{p_i\in\Omega}\rho\big(I(p_i + V(p_i,t),t+1) - I(p_i,t),\sigma\big) = \\ = \sum_{p_i\in\Omega}\rho\big(r(p_i + V),\sigma\big) \tag{25}$$

and the motion wavelet coefficient vector, θ, is calculated by:

$$\theta = \arg\min_{\theta}(E) \tag{26}$$

Once motion wavelet coefficients have been estimated for each frame f_i of a sequence S containing M frames, anyone can obtain a feature space spanned by the motion feature vectors θ_i, i = 1, ... M. To temporally segment the feature spaces Ω_{seg} (spanned by θ_{seg}), (Bruno & Pellerin, 2002) consider a hierarchical classification with a temporal connexity constraint.

Another approach is only formally different (Wu et al, 1998). Approximation of motion vector, $\theta = [u(x,y)\ \ v(x,y)]^T$, by using two-dimensional basis functions, is a natural extension of one-dimensional to two-dimensional basis functions of the tensor product. Accordingly, the two-dimensional basis functions are:

$$\Phi_{0,k_1,k_2}(x,y) = \phi(x-k_1)\phi(y-k_2) \tag{27}$$

$$\Psi^{H}_{j,k_1,k_2}(x,y) = \phi(2^j x-k_1)\psi(2^j y-k_2) \tag{28}$$

$$\Psi^{V}_{j,k_1,k_2}(x,y) = \psi(2^j x-k_1)\phi(2^j y-k_2) \tag{29}$$

$$\Psi^{D}_{j,k_1,k_2}(x,y) = \psi(2^j x-k_1)\psi(2^j y-k_2) \tag{30}$$

where the subscripts j, k_1 and k_2 represent the resolution scale, horizontal and vertical translations and the upper subscript H, V and D represent the horizontal, vertical and diagonal directions. Two dimensional motion vector can be expressed in terms of linear combinations of coarsest-scale function (13) and horizontal, vertical and diagonal wavelets (14 - 16) in finer levels. Motion vectors are (Wu, 1998):

$$u(x,y) = u_{-1}(x,y) + \sum_{,j=0}^{J}\left(u^{H}_{j}(x,y) + u^{V}_{j}(x,y) + u^{D}_{j}(x,y)\right) \tag{31}$$

$$v(x,y) = v_{-1}(x,y) + \sum_{,j=0}^{J}\left(v^{H}_{j}(x,y) + v^{V}_{j}(x,y) + v^{D}_{j}(x,y)\right) \tag{32}$$

where u_{-1} is:

$$u_{-1}(x,y) = \sum_{k_1=-2}^{L_1-2}\sum_{k_2=-2}^{L_2-2} c_{-1,k_1,k_2}\Phi_{0,k_1,k_2}(x,y) \tag{33}$$

where u_j in all directions is expressed as:

$$u^{H,V,D}_{i} = \sum_{k_1=-2}^{2^j L_1-2}\sum_{k_2=-2}^{2^j L_2-2} c^{H,V,D}_{j,k_1,k_2}\Psi^{H,V,D}_{j,k_1,k_2}(x,y) \tag{34}$$

v_{-1} and v_i are calculated analogly. Maximum likehood estimates $[u(x, y)\ v(x, y)]^T$ are obtained by minimizing:

$$E = \sum_{x}\sum_{y}\left[I_1(x+u(x,y), y+v(x,y)) - I_0(x,y)\right]^2 \tag{35}$$

Equations (31 – 35) are easier for implementation than (23 – 26). They can be approximated as differences of neighbouring approximation, diagonal, vertical and horizontal coefficients. This approximation is used in quasi-superresolution algorithm (Vujović et al., 2006a; Vujović et al., 2006b).

3.2. Superresolution and quasi-superresolution

Superresolution includes restoration as a special case. The restoration equation can be rewritten within the superresolution framework as (Nguyen & Milanfar, 2000):

$$f_k = DC_kE_kx + n_k = H_kx + n_k \tag{36}$$

where p is the number of available frames and $1 \le k \le p$, f_k is an N x 1 vector representing the k^{th} m x n LR image in columnwise order. If l is the resolution enhancement factor in each direction, x is an l^2N x l vector representing the lm x ln HR image in columnwise order, E_k is an l^2N x l^2N warping matrix that represents the relative motion between frame k and a reference frame, C_k is a blur matrix of size l^2N x l^2N, D is the N x l^2N uniform down-sampling matrix, and n_k is the N x 1 vector representing additive noise. Particularly in case of quasi-superresolution, only one image is available (k = 1). Than, superresolution problem can be replaced with filtering and (36) transforms to:

$$f = DCEx + n = Hx + n \tag{37}$$

Since, only in ideal case n = 0, (37) means that HR image is "less clear", which is totally subjective description.

3.3. Algorithm flow

The input image can be processed by morphology operations, but it is optional (block 1 in Fig. 4).

Noise reduction is in the nature of WT, so it is not included in the algorithm. It is also possible to combine the original and processed image. Then it must be chosen which transformation to use (filter or lifting approach). WT is performed between blocks 3 and 4.

Thresholding can be performed if necessary as the preprocessing for the compression or simple for denoising. This option can be performed automatically or manual. Next step is to enhance image incorporating wavelet motion field. When dealing with stationary stand alone image (i.e. in biomedical diagnostic images such as X-rays), motion field calculation is performed in quasi-superresolution manner (Vujović et al, 2006a). This is relative "motion" between wavelet coefficients. In on-line sequences quasi-superresolution can be performed when higher image resolution is necessary and motion can be resolved in some other way if someone do not prefer wavelet motion field. Then we can perform what we need. Edges are obtained by adding all four motion matrixes obtained in quasi-superresolution manner.

When approximation is down-sampled several times and reducing number of colours edges can be pointed out as well. When subtraction of motion matrixes from the enhanced original (previous steps) is performed, a good segmentation is obtained. If enhanced original is put through quasi-superresolution algorithm, HR image can be obtained.

Compression of images can be performed with or without reconstruction at HR grid. Compression can be obtained by thresholding of wavelet coefficients or by downsampling of wavelet coefficients. Multiple downsampling is proven to be useful for compression

(Vujović, 2004) in case study about pulmonary X-rays, when downsampling is performed 6 to 12 times without influence to the medical diagnosis. Of course, it is not generalized.

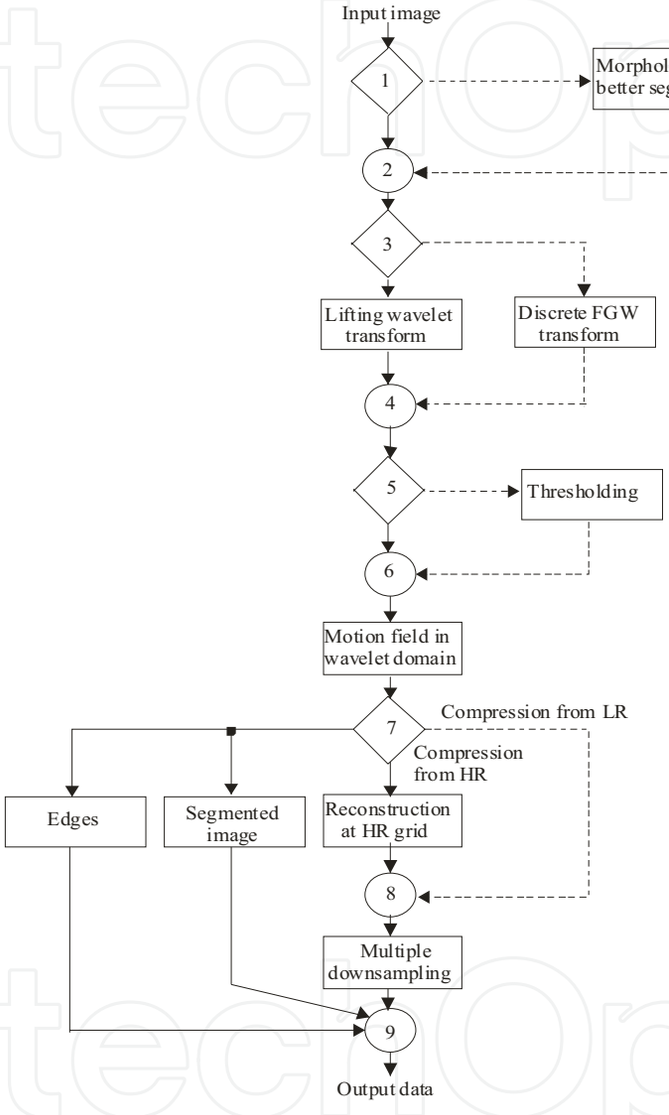

Fig. 4. Flexible algorithm for wavelet segmentation, edge detection and compression

4. Results

Times of execution depend from computer to the computer, so it is very difficult to compare. We executed algorithm on NEC notebook with Athlon XP-M AMD processor with 1.67 [GHz] and 480 [MB] RAM size with Windows XP operating system. Hard disk is half full and Norton Antivirus is active.

Fig. 5. Motion field execution on wavelet coefficients in stand alone image with quasi-superresolution reconstruction to HR grid

Type of wavelets (Matlab designation)	Time of execution of filtered WT [s]	Time of execution of lifted WT [s]	Improvement in percentage [%]
bior1.3	12.768	11.978	6.18
rbio1.3	12.598	12.528	0.55
haar	12.128	11.536	4.88

Table 1. Comparison of wavelet quasi-superresolution execution time

Fig. 5 to 12 shows some of the results. Figures are chosen to open discussion. There are better and worse examples.

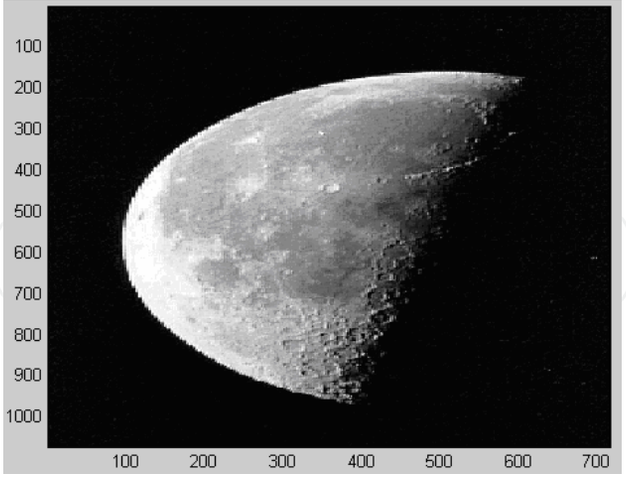

Fig. 6. Reconstruction after wavelet motion field for FGW haar

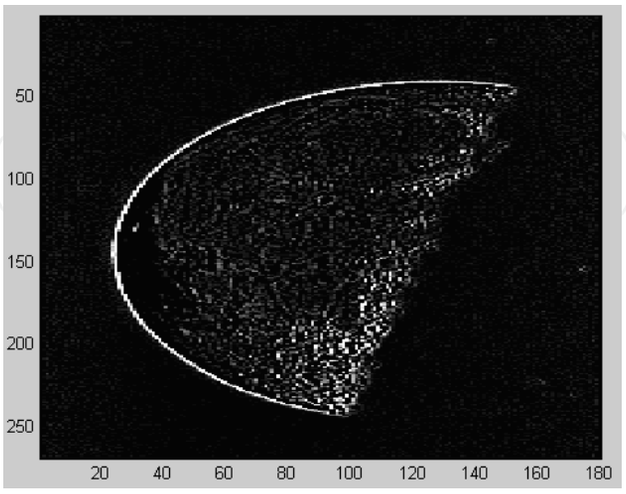

Fig 7. Simple edge detection by usage of only motion field vectors without the original from downsampled approximation coefficients

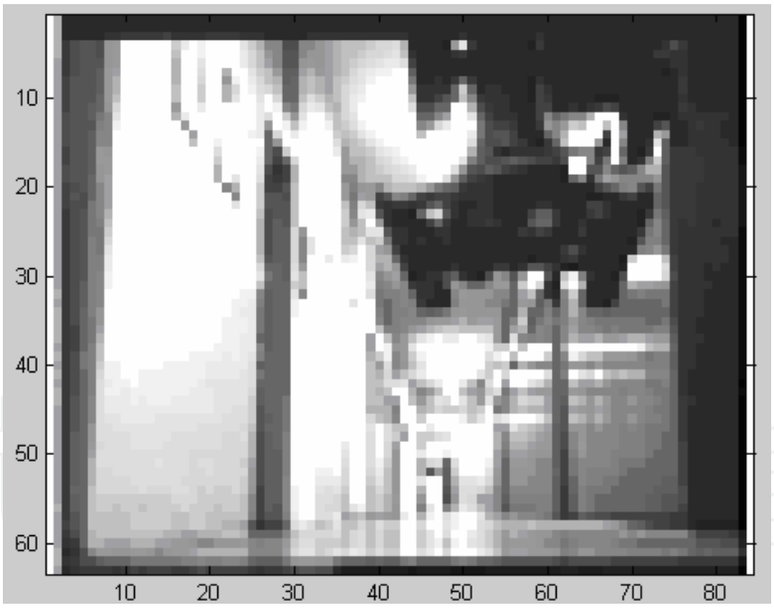

a)

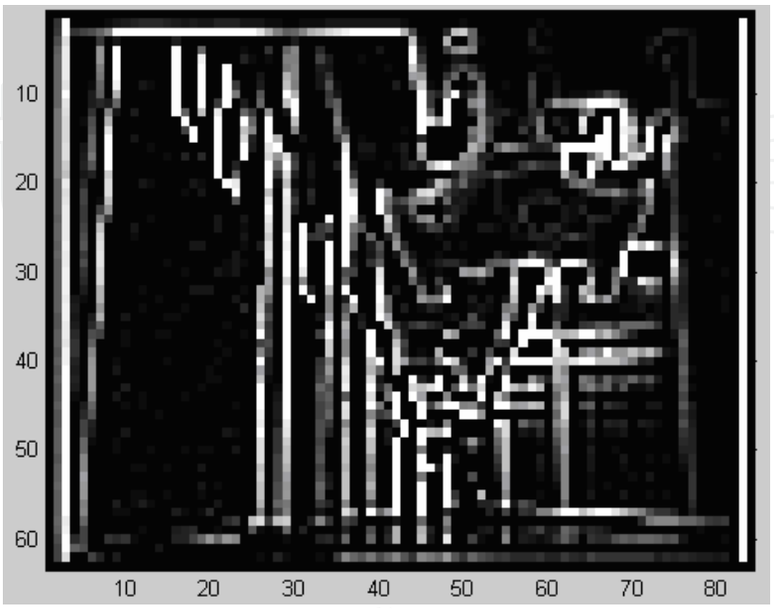

b)

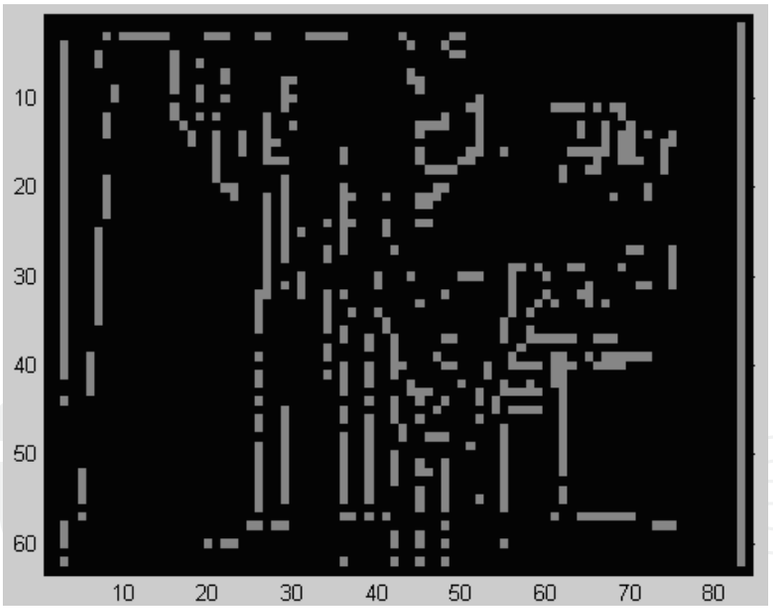

c)

Fig. 8. A robot perspective: a) original image, b) edge detection by wavelet motion vectors with the original colour map, c) edge detection by wavelet motion vectors with the increased number of colours

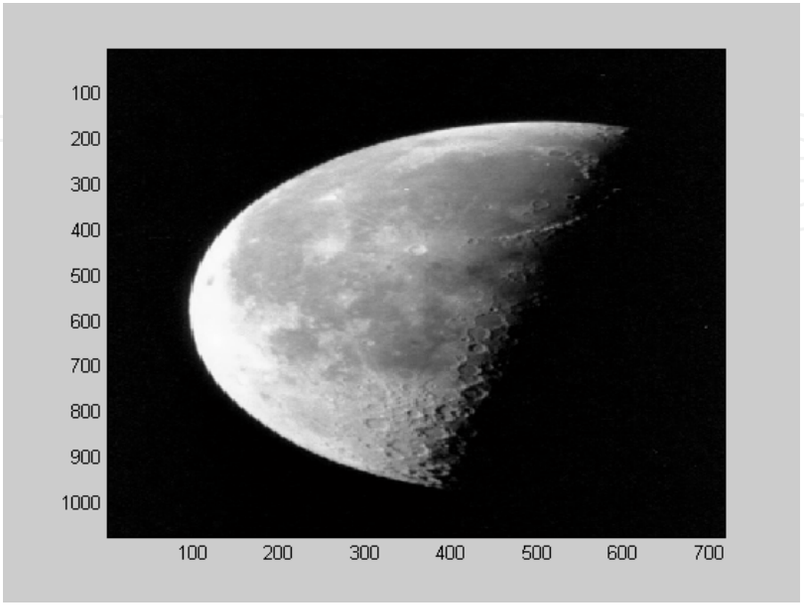
100
200
300
400
500
600
700
800
900
1000
100
200
300
400
500
600
700

a)


100
200
300
400
500
600
700
800
900
1000
100
200
300
400
500
600
700

b)

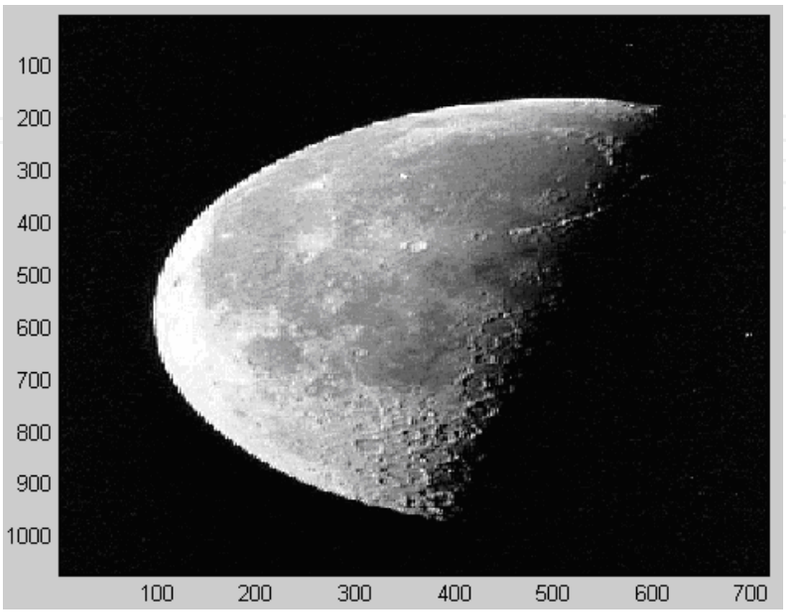

c)

Fig. 9. a) Classic zoom of the approximation, b) quasi-superresolution on approximation with FGW, c) quasi-superresolution on approximation by SGW

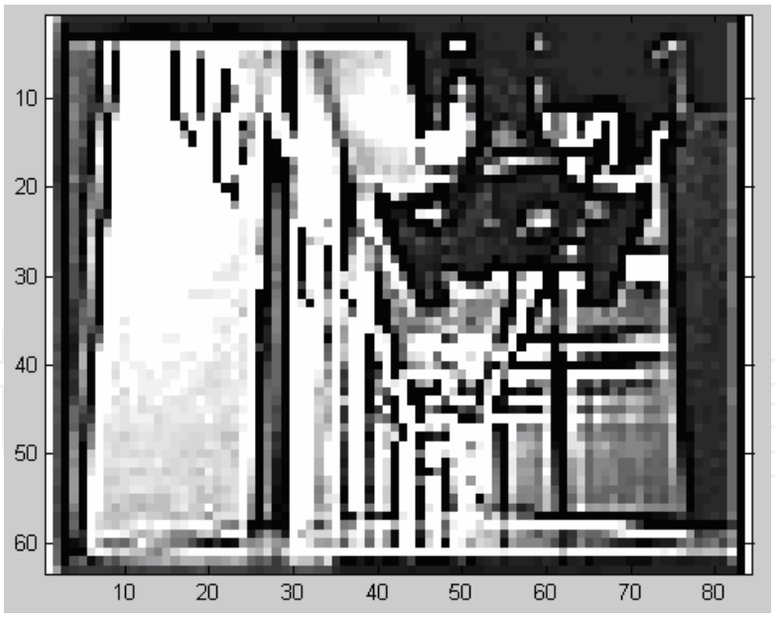

a)

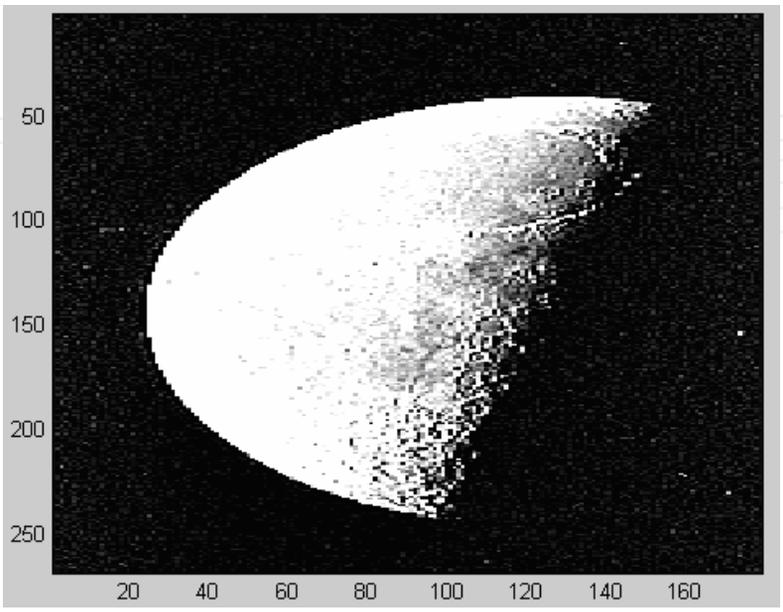

b)

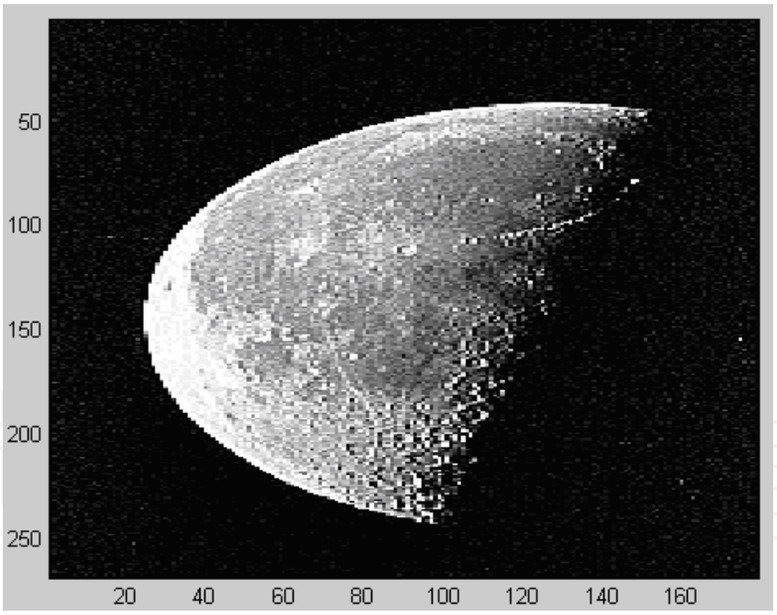

c)

Fig. 10. Addition of motion fields in all directions subtracted from the approximation at the first level: a) robot's view, b) lifting WT, db2, c) lazy wavelet

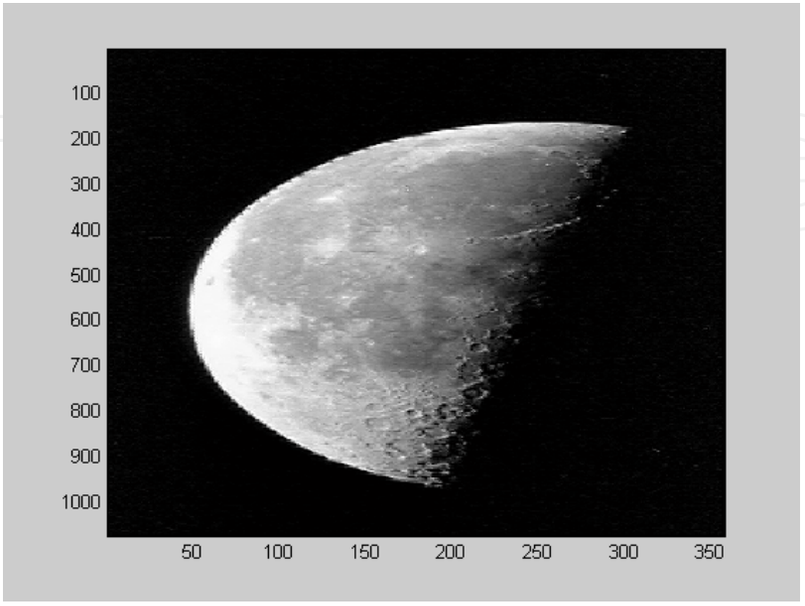
100
200
300
400
500
600
700
800
900
1000
50
100
150
200
250
300
350

a)

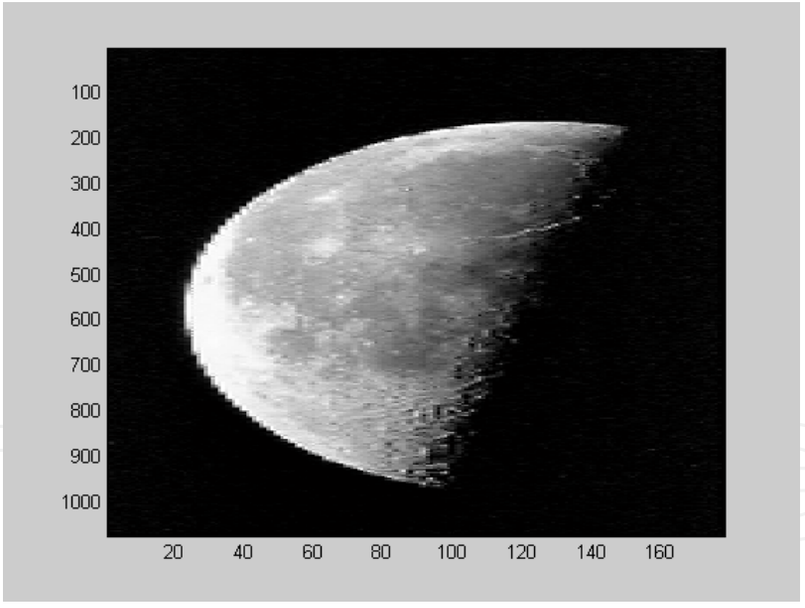
100
200
300
400
500
600
700
800
900
1000
20
40
60
80
100
120
140
160

b)

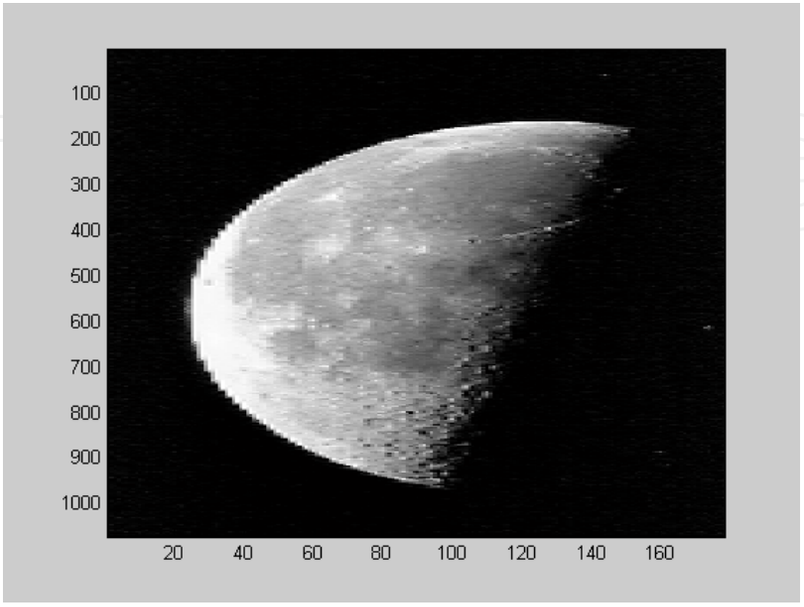

c)

Fig. 11. Image reconstructed from: a) down-sampled original (motion-vector enhanced before), coefficients were not up-sampled (IDWT, db2), b) twice down-sampled original (motion-vector enhanced), not up-sampled coefficients (IDWT, db2), c) twice down-sampled original (motion-vector enhanced) and not up-sampled coefficients before (ILWT, db2)

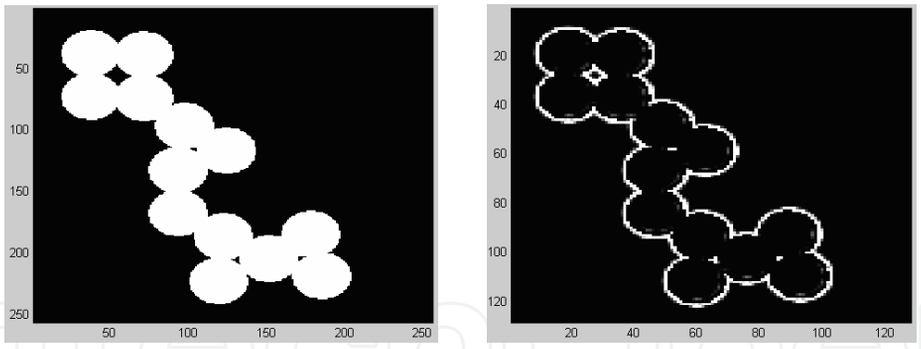

a) b)

Fig. 12. a) Original image, b) wavelet motion field edge detection

5. Example in medical imaging (Vision system for X-rays)

One of applications of vision systems is in medicine. Every modern hospital has Hospital Information System (HIS) or Picture Archiving and Compression System (PACS) at least in rudimental way. Telemedicine is old news. Our research started with compression of pulmonary X-rays for asbestosis infected patients. The problem was how to compress images without changing the diagnosis. In (Vujović, 2004) the goal is reached for lossy

compression by down-sampling. Images were degraded in quality, but diagnostic value is preserved. Compression ratio obtained was 1:128 or higher (depending on type of wavelets). This was confirmed by three independent medical experts, as required by International Labour Organization.

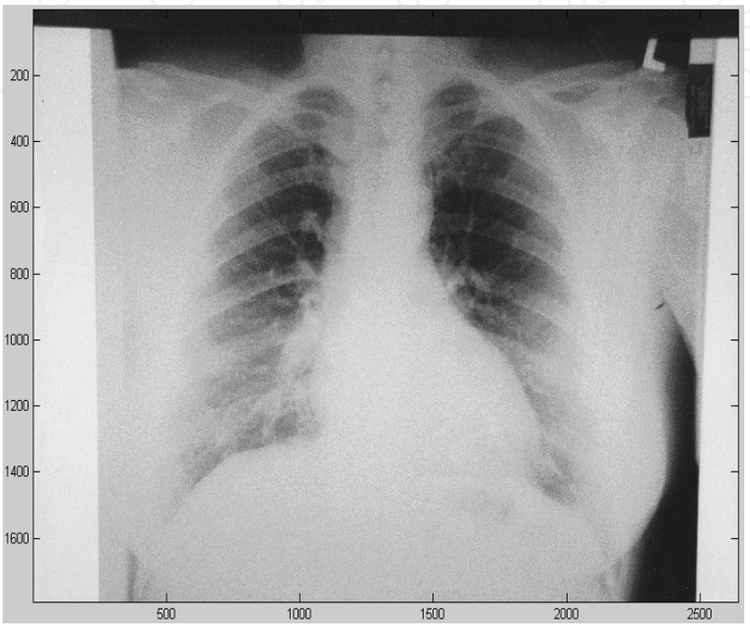

a)

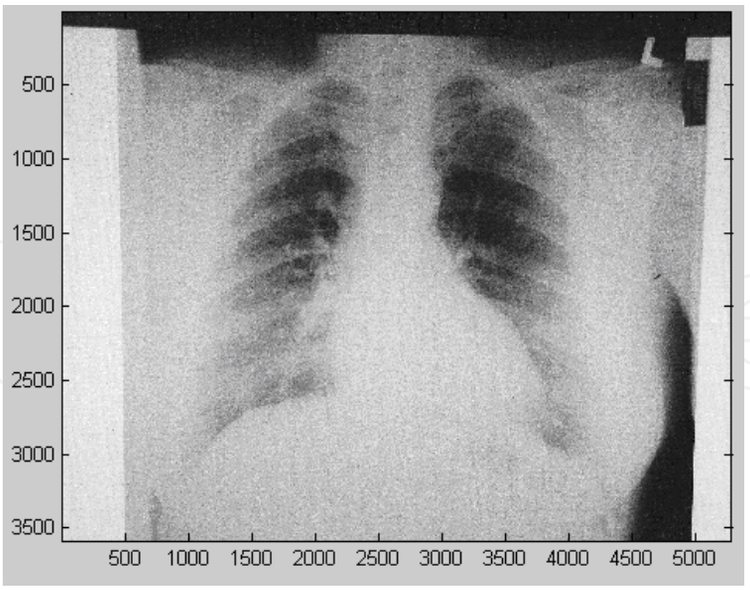

b)

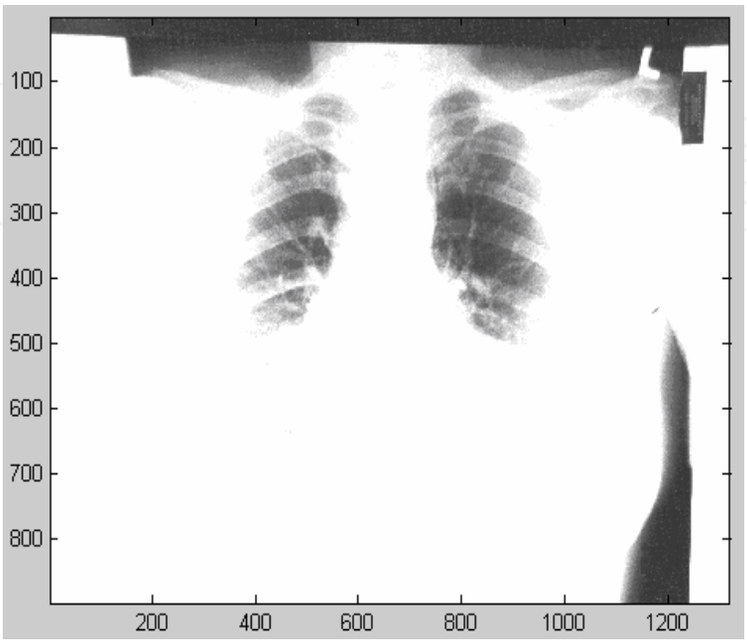

c)

Fig. 13. a) Original X-ray of randomly chosen patient, b) motion field in wavelet domain (quasi- superresolution), c) approximation coefficients

Fig. 13.a shows original of randomly chosen patient. In Fig. 13.b motion-field enhanced, quasi-superresolution image is shown. Fig. 13.c shows approximation coefficients. Fig. 14. shows results on compression for wavelet motion field enhanced X-rays. Compression ratio for lossless compression is 1 : 8.0211 in Fig. 14.d and 1 : 4.0189 for Fig. 14.c.

Superresolution and quasi-superresolution are, in nature, processes of obtaining higher resolutions and more details. The question in this case is what do the new details mean. Can it be beginning useful in prevention of diseases by early diagnosis (when medical experts still can not see the illness)? Or is it a cause of error, because the new details do not mean illness. The new details could be only math creation without meaning in nature. Which of this is true? The second danger is in thresholding, because small shadows (which mean illness) can be deleted if not carefully used. Medical diagnosis is not changed in such compression as illustrated.

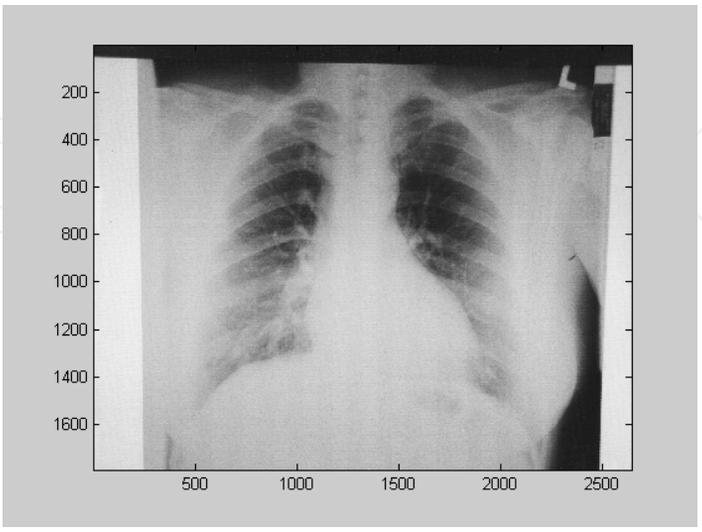
200
400
600
800
1000
1200
1400
1600
500
1000
1500
2000
2500

a)

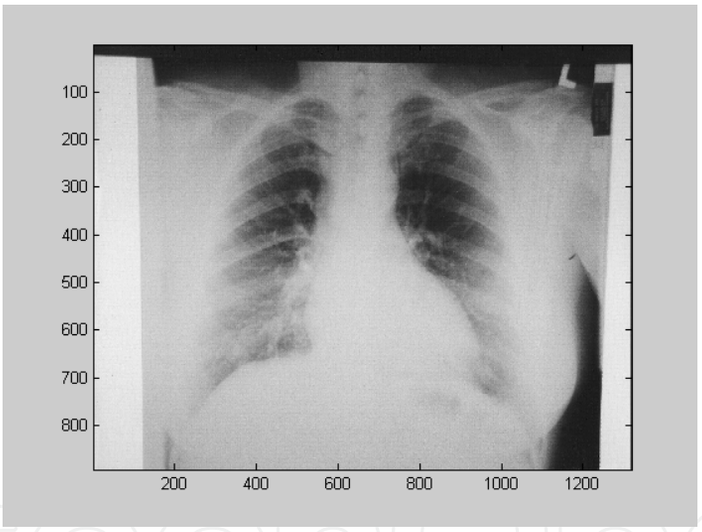
100
200
300
400
500
600
700
800
200
400
600
800
1000
1200

b)

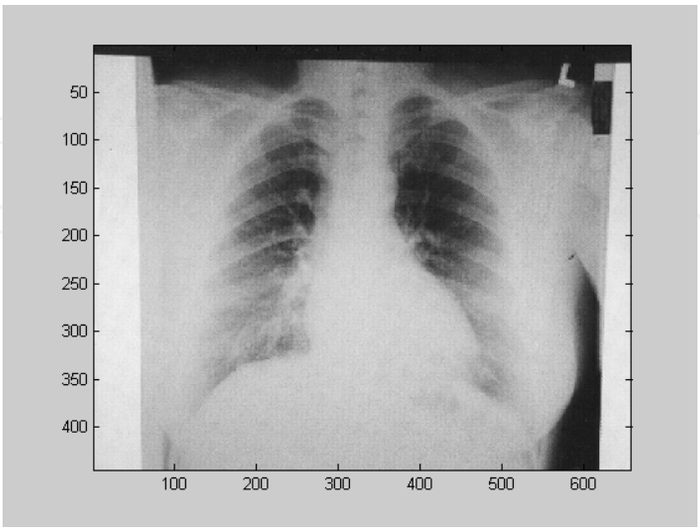

c)

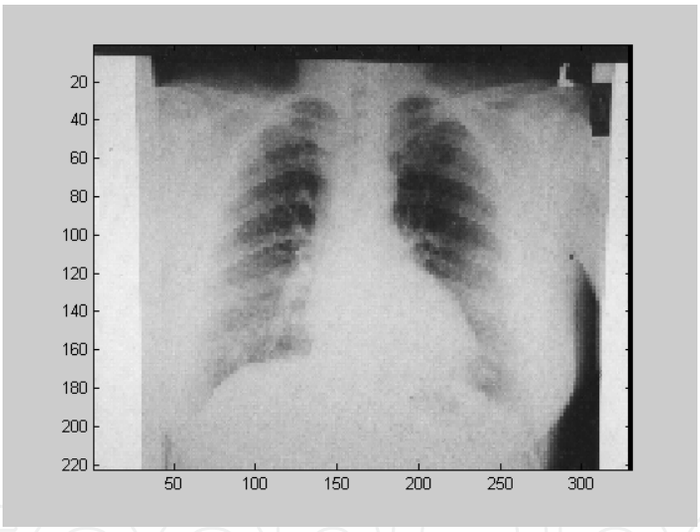

d)

Fig. 14. a) Original X-ray, b) image down-sampled two times after wavelet motion field enhancement , c) image down-sampled three times after wavelet motion field enhancement, d) image down-sampled four times after wavelet motion field enhancement

6. Conclusion

Wavelets have evolved over years. FGW and SGW are still used and they are applied in more and more areas of research. Proposed algorithm is flexible, because of many options which can be used. It can be simple, but also complex. Disadvantage of many image

processing algorithms is that they do not give the same results on every class of images. So, they are not generalized. This algorithm has the same fate. It gives the best results for pulmonary X-rays with gray scale.

Time of execution is with active Norton Antivirus in Windows and Matlab with half-full hard disk. It would be considerable faster if it is executable stand alone application isolated and without antivirus application. There are a lot of programming solutions to make faster the algorithm. Since it is still in developing phase, we had the main interest in operation algorithm. Further work should include improvement of execution time.

Potential area of application is biomedical imaging, because there is no need to take care of execution time. However, it could be used in virtual reality systems and systems of augmented reality. This is possible, because it is not necessary to execute the algorithm in real-time all the time. Algorithm can be performed occasionally, i.e. when scene is changed. In the meantime, only differences in frames can be processed. This can be improved by choosing only limited regions of interest for processing.

It is important not to mix up motion field in an image sequence and in a stationary image. Motion field in the image sequence is defined as in section 3.1. Motion field in the stationary image is without sense, because there are no two frames to look for motions. However, quasi-superresolution states that we can find motion between neighbouring wavelet coefficients. So, this motion does not correspond to real motion in the observed scene. This is a novel idea, which helps in i.e. medical imaging, finger print analysis, human iris recognition, face recognition, etc. Fig. 12. shows potential of wavelet motion vectors in edge detection. Further research should be inclusion of colours and colour segmentation.

Vision systems in medicine must be carefully used, because of misdiagnosis danger. I.e. in superresolution, when an un-seen detail shows up, it could mean that illness is discovered before medical expert could see it. But, it can be a false positive. If a vision system is used instead, the system must be checked by medical experts for any possible case. The algorithm could be incorporated in computer hardware and sell as medical vision system. It has to be checked by appropriate bodies in different countries before.

7. References

Abbas, Y & Alsultanny, K. (2005). Edge Defection Prediction by Using Wavelet Compression. *Journal of Computer Science*, Vol. 1., No. 3., pp. 310-315, ISSN 15493636

Akay, M. (Ed.) (1998). *Time Frequency and Wavelets in Biomedical Signal Processing*, IEEE Press, Piscataway, ISBN 0-7803-1147-7, New York

Arsenio, A. M. (2003). Object Segmentation Through Human-Robot Interactions in the Frequency Domain. On-line: www.groups.csail.mit.edu/lbr/hrg/2003/arsenio_sib.pdf (URL last checked on December 2006)

Boles, W. W. (1998). A Security System Based on Human Iris Identification Using Wavelet Transform. *Engineering Applications of Artificial Intelligence,* Vol. 11., No. 1., pp. 77-85 ISSN 0952-1976

Borman, S. (2004). *Topics in Multiframe Superresolution Restoration*, PhD Thesis, University of Notre Dame, Indiana, USA

Bose, N. K. (2003). *Iterative Blind Second Generation Wavelet Superresolution and Role of Moving Least Squares*, Pennstate University, Army Research Office Grant DAAD 19-03-1-0261, Presentation.

Bruno, E. & Pellerin, D. (2002). Video Structuring, Indexing and Retrieval Based on Global Motion Wavelet Coefficients. *Proceedings of International Conference of Pattern Recognition* (ICPR), pp. 132-137, ISBN 0-7695-1695-X, Quebec City, Canada, 11-15. August 2002, IEEE Computer Society Press, Piscataway

Bruno, E. & Pellerin, D. (2001). Global Motion Model Based on B-spline Wavelets: Application to Motion Estimation and Video Indexing. *Proceedings of the 2nd Int. Symposium on Image and Signal Processing and Analysis ISPA'01*, pp. 102-107, S. Lončarić, H. Babić (Ed), Pula, Croatia, June 2001

Calderbank, A. R.; Daubechies, I.; Sweldens, W. & Yeo, B. L. (1997). Lossless Image Compression Using Integer to Integer Wavelet Transforms, *Proceedings of International Conference on Image Processing ICIP,* Vol. 1, pp. 596-599, ISBN 0-8186-8183-7, Washington, DC, USA, 26-29th October 1997.

Candocia, F. M. (1998). *A Unified Superresolution Approach for Optical and Synthetic Aperture Radar Images*, PhD Thesis, University of Florida.

Chan, D. Y.; Lin, C. H. & Hsieh, W. S. (2005). Image Segmentation with Fast Wavelet-Based Colour Segmenting and Directional Region Growing. *IEICE Transactions on Information & Systems*, Vol.E88–D., No.10., pp. 2249-2249, ISSN 0916-8532

Chappalli, M. B. & Bose, N. K. (2005). Simultaneous Noise Filtering and Super-resolution with Second Generation Wavelet. *IEEE Signal Processing Letters*, Vol. 12., No.11., pp. 772-775, ISSN 1070-9908

Dai, D. Q. & Yuen, P.C. (2006). Wavelet Based Discriminant Analysis for Face Recognition. *Applied Mathematics and Computation*, Vol. 175., No. 1., pp. 307–318, ISSN 0096-3003

Daubechies, I. & Sweldens, W. (1998). Factoring Wavelet Transforms Into Lifting Steps. *Journal of Fourier Analysis Applications*, Vol. 4., No. 3., pp. 247-269, ISSN 1069-5869

Grosbois, R. (2003). *Image Security and Processing in the JPEG 2000 Compressed Domain.* PhD Thesis, Université Paris, France

Heer, V. K. & Reinfelder, H-E. (1990). A Comparison of Reversible Methods for Data Compression. *Proceedings of SPIE "Medical Imaging IV"*, SPIE, Vol. 1233, pp. 354-365, ISBN 0-8194-0277-X

Jansen, M. & Oonincx, P. (2005). Second Generation Wavelets and Applications, Springer-Verlag, ISBN 1-85233-916-0, London

Jiang, X. Q. & Blunt, L. Third Generation Wavelet Model for Surface Texture. *Proceedings of 9th International Conference on Metrology and Properties of Engineering Surface*. Halmstad University, Sweden, 10-11 September 2003. ISBN 91-631-5455-2

Mallat, S. (1999). *A Wavelet Tour of Signal Processing* 2nd Edition. ISBN 0-12-466606-X Academic Press, London, UK

Mertins A. (1999). *Signal Analysis: Wavelets, Filter Banks, Time-Frequency Transforms and Applications* .John Wiley & Sons Ltd., ISBN 0-471-98627-7, Baffins Lane, Chichester, West Sussex, England

Nguyen, N. X. (2000). *Numerical Algorithms for Image Superresolution*. PhD Thesis, Stanford University, USA

Nguyen, N. & Milanfar, P. (2000). A Wavelet-Based Interpolation-Restoration Method for Superresolution, on line: www_sccm.stanford.edu/pub/sccm/sccm00-03.ps.gz (URL last checked, June 2006)

Proakis G. J. & Manolakis G. D. (2006). *Digital Signal Processing, Principles, Algorithms, and Applications.* 4th Ed., Pearson Prentice Hall Inc., ISBN 0-13-187374-1, Upper Saddle River, NJ, USA

Said, A. & Pearlman, W. A. (1996). An Image Multiresolution Representation for Lossless and Lossy Compression. *IEEE Transactions on Image Processing*, Vol. 5., No. 9., pp. 1303-1310, ISSN 1057-7149

Šoda, J. (2005). *Time-frequency Analysis of Measured Signal.* (In Croatian). Master Thesis, University of Split, Faculty of Electrical Engineering, Mechanical Engineering and Naval Architecture, Split, Croatia

Sweldens, W. (1996). The Lifting Scheme: A Custom-design Construction of Biorthogonal Wavelets. *Application of Computer Harmoning Analysis*, Vol. 3., No. 2, pp. 186-200

Vetterli M. & Kovačević J. (1995). *Wavelets and Subband Coding.* Prentice-Hall Signal Processing Series. ISBN 0-13-097080-8, London, UK

Vujović, M.; Vujović, I. & Kuzmanić, I. (2003). The Application of New Technologies in Diagnosing Occupational Asbestosis. *Arhiv za higijenu rada i toksikologiju*, Vol. 54., No. 4., pp. 245-252, ISSN 0004-1254

Vujović, I. (2004). Application of Wavelets in Biomedical Signal Processing with Example in Compression of X-ray Images of Occupational Asbestosis Infected Patients. (in Croatian). *Master Thesis,* University of Split, Faculty of Electrical Engineering, Mechanical Engineering and Naval Architecture, Split, Croatia.

Vujović, I.; Kuzmanić, I. & Vujović, M. (2006.a). Algorithm for Combined Wavelet Quasi-Superresolution. *Proceedings of 5th Int. Symposium Communication Systems Networks and Digital Signal Processing*, pp. 469-473, ISBN 960-89282-0-6, Patras, Greece, 19-21 July 2006, CSNDSP, School of CEIS, Northumbria University, Newcastle upon Tyne

Vujović, I.; Kuzmanić, I. & Kezić, D. (2006.b). Wavelet Superresolution and Quasi-Superresolution in Robot Vision. *Proceedings of 10th International Research/Expert Conference "Trends in the Development of Machinery and Associated Technology"* TMT-2006, pp. 597-600, ISBN 9958-617-30-7, Barcelona-Lloret de Mar, Spain, 11-15th September 2006., Publishers: Faculty of Mechanical Engineering, Zenica, Bahçeşehir University Istanbul, Mühendislik Fakültesi, Turkey, Escola Tecnica Superior D'Enginyeria Industrial de Barcelona, Universitat Politecnica de Catalunya, Zenica, Barcelona, Istambul

Wichmann, E. H. (1988). *Quantum physics.* Textbook from University of Berkeley (translation to Croatian). ISBN 86-7059-056-5, Tehnička knjiga, Zagreb, Croatia

Wu, Y. T.; Kanade, T.; Cohn, J. & Li, C. C. (1998). Optical Flow Estimation Using Wavelet Motion Model. *Proceedings of 6th IEEE International Conference on Computer Vision*, pp. 992-998, Bombay, India, 4-7 January 1998.

Xiao, S. J.; Jiang, X. Q. & Blunt, L. (2003). Wavelet Bayesian Method for Denoising of Nano-scalar Surface Measurement. *The International Journal for Manufacturing Science & Production*, Vol. 5, No. 1-2., pp. 95 – 98, ISSN 0793-6648

Vision Systems: Segmentation and Pattern Recognition
Edited by Goro Obinata and Ashish Dutta

ISBN 978-3-902613-05-9
Hard cover, 536 pages
Publisher I-Tech Education and Publishing
Published online 01, June, 2007
Published in print edition June, 2007

Research in computer vision has exponentially increased in the last two decades due to the availability of cheap cameras and fast processors. This increase has also been accompanied by a blurring of the boundaries between the different applications of vision, making it truly interdisciplinary. In this book we have attempted to put together state-of-the-art research and developments in segmentation and pattern recognition. The first nine chapters on segmentation deal with advanced algorithms and models, and various applications of segmentation in robot path planning, human face tracking, etc. The later chapters are devoted to pattern recognition and covers diverse topics ranging from biological image analysis, remote sensing, text recognition, advanced filter design for data analysis, etc.

InTech Europe
University Campus STeP Ri
Slavka Krautzeka 83/A
51000 Rijeka, Croatia
Phone: +385 (51) 770 447
Fax: +385 (51) 686 166
www.intechopen.com

InTech China
Unit 405, Office Block, Hotel Equatorial Shanghai
No.65, Yan An Road (West), Shanghai, 200040, China
中国上海市延安西路65号上海国际贵都大饭店办公楼405单元
Phone: +86-21-62489820
Fax: +86-21-62489821

IntechOpen